

CHARACTERISTICS OF PF LINAC INJECTION SYSTEM

A. Asami, S. Ohsawa, T. Shidara, T. Urano and J. Tanaka

National Laboratory for High Energy Physics
Oh-machi, Tsukuba-gun, Ibaraki-ken, 305, Japan

T. Ozaki

Nihon University
Surugadai, Chiyoda-ku, Tokyo, 101, Japan

ABSTRACT

An electron gun and associated circuit system have been developed to supply electron beams with a long ($\sim 1 \mu\text{s}$) or short ($\sim 1.5 \text{ ns}$) duration to PF ring and TRISTAN accumulation ring. Switching over from one to the other duration mode is made in a moment to enable simultaneous operation of these two rings. Beam characteristics in a stationary state were studied by measuring bunch widths and energy spectra. The variation of the bunch width was measured with the variation of prebuncher rf power, buncher rf phase and injection current. The energy spectrum was measured as a function of injection current.

INTRODUCTION

The PF linac had been extensively used to accelerate electrons up to 2.5 GeV and inject them into the PF storage ring. In October 1984, the construction of the TRISTAN accumulation ring (AR) was completed and test operation started. Since then the linac has been operated as an injector of the AR as well.

Beam characteristics required for the AR is different from those required for the PF, i.e., the beam pulse width for the PF is a few hundreds nanoseconds to one microsecond, whereas that for the AR is less than two nanoseconds. To meet these requirements, a short pulse grid pulser and a small jitter triggering system using an optical fiber has been developed. In addition, a fast switching system from a long/short pulse to a short/long pulse operation mode was also made to enable simultaneous operation of both rings.

The beam bunch width was measured as a function of the buncher rf phase and the injection current from the gun. The variation of the energy spectrum was measured with the variation of the injection current.

ELECTRON GUN AND ASSOCIATED CIRCUIT SYSTEM¹

Grid Pulser

A grid pulser was fabricated and tested to produce a beam with a width of less than 2 nsec. The circuit diagram is shown in Fig. 1, where the fast pulse is produced by discharging the stored charge in a short coaxial cable of 10 cm long. The discharge is done by

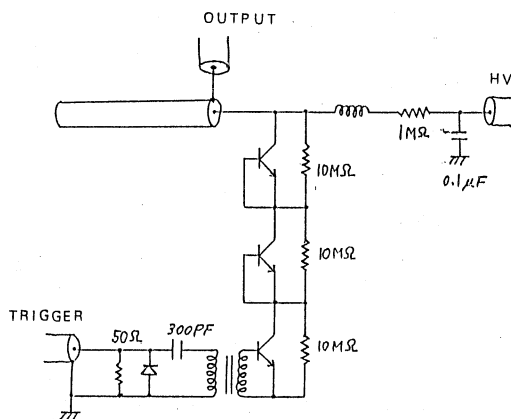
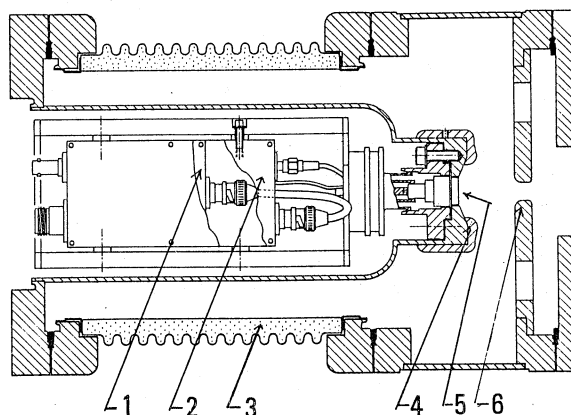


Fig. 1 Grid pulser.

switching on three cascade avalanche transistors. The pulse thus formed has an amplitude of 130 volts and a FWHM of 1.8 nsec.

Trigger Circuits²

To transmit a trigger signal to the grid pulser of the gun installed at high potential, an optical fiber seems to be most suited because there is no insulation problem and it is easy to handle. A time jitter, however, is most significant problem and a special care must be paid in transmitting fast signals. The trigger signal transmission system fabricated consists of an electric to optical signal conversion circuit with a laser diode and optical fiber of 20 m long, and an optical to electric signal (O/E) conversion circuit with a PIN photodiode. Time jitter less than 30 ps was achieved.



(1) O/E module (2) grid pulser (3) ceramic insulator
(4) focussing electrode (5) cathode grid assembly
(6) anode

Fig. 2 Electron gun assembly.

The O/E conversion circuit is installed inside of the ceramic insulator of the gun together with the grid pulser for short pulse operation as shown in Fig. 2. The distance between the output of the grid pulser and the grid cathode assembly of the gun is thus kept minimum.

Switching System

The trigger signal is usually synchronized to the rf and revolution frequencies of the storage or accumulation ring in order to stack electrons in a definite bunch or bunches in the ring. Trigger circuits and grid pulsers for a long and a short pulse operation are both connected to the gun with a small inductance between the output of the long grid pulser and the gun. An operation mode of a long pulse or a short pulse beam is determined by selecting which of the trigger circuits is actuated. The selection is done by a push-button in a moment. The small inductance works as a low pass filter, and affects little on the output of the long pulse signal.

Performance

Figure 3 shows a beam signal observed at the end of the linac where the beam energy reaches about 2.5 GeV. The observation was made with a monitor³ of wall current detection type and a cable of 10 m long, and this measurement showed that the peak current is about 110 mA, and the FWHM is less than 1.5 ns. The overall time jitter of the beam signal to the trigger signal was measured on a scope and found to be much less than 100 ps.

When the beam is injected into the AR or PF ring, a single bunch of the beam was successfully obtained in both rings. Figure 4 shows a single bunch beam first observed in the PF ring in Dec. 1983.

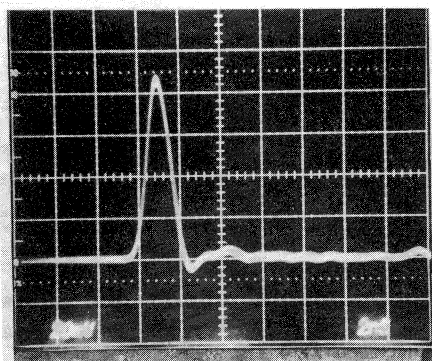


Fig. 3 Short pulser beam shape.

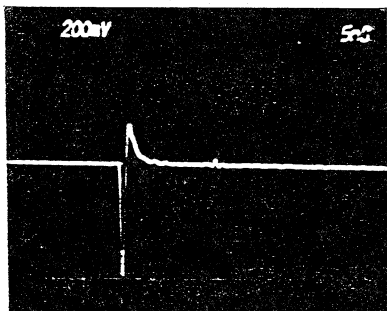


Fig. 4 Single bunch beam in PF ring.

BEAM CHARACTERISTICS⁴

Bunch Width

Bunch width measurements were made with the method described in ref. 5, and here stated briefly, the width is estimated from the energy spread of the beam with a special procedure to reduce the relative energy spread arising from other reasons than the finite bunch width.

First, the variation of the bunch width was studied with the variation of prebuncher rf power and buncher rf phase and the results were shown in Figs. 5 and 6. The bunch width is mainly determined by the buncher, and the width at prebuncher rf power being zero corresponds to that due to the buncher itself. When the rf power is increased from zero, the width rapidly reduces to 1 or 2 degrees. This shows that weak prebunching is enough for the buncher to make a well bunched beam, suggesting the buncher has a large acceptance phase angle. The bunch width remains constant when the buncher rf phase is varied by as much as 30°. To change the buncher rf phase means to change not only the prebuncher rf phase but also that of the two accelerator guides following the buncher. At the optimum rf phase for the buncher, the beam is at the rf crest of the accelerator guides, so that the bunch may

be insensitive to the variation of the rf phase. The bunch width is also measured when the injection current from the gun is changed. The result is shown in Fig. 7, the width does not depend on the current at least in the region tested.

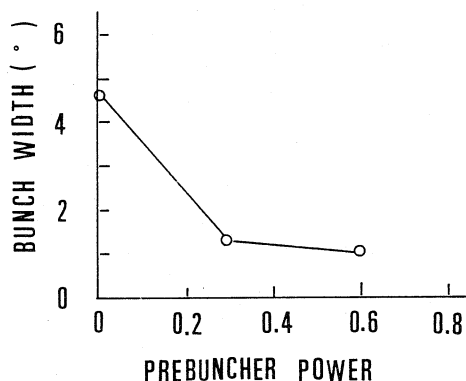


Fig. 5 Bunch width versus prebuncher rf power.

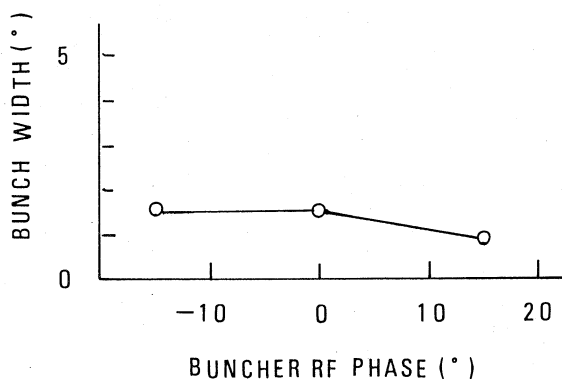


Fig. 6 Bunch width versus buncher rf phase.

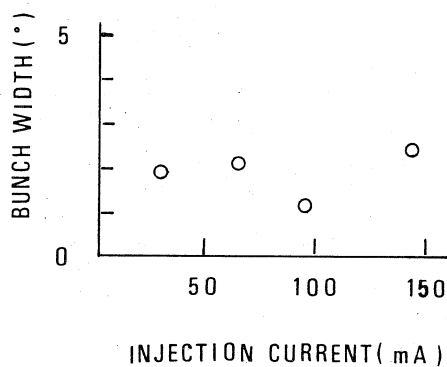


Fig. 7 Injection current dependence of bunch width.

Energy Spectra

Using an energy analyzing system installed at the end of the injector, energy spectra were measured as a function of injection current. The analyzing system consists of a 45° deflection analyzing magnet, a slit and a beam catcher. When the injection current is changed, the transport elements were readjusted to obtain an optimum transmission. The result is shown in Fig. 8, where the parameter is the injection current from the gun. The beam current is normalized to unity at the peak to show the shape of spectrum more clearly. The peak energy decreases linearly with the increase of injection current with a gradient of 0.3 MeV/10 mA.

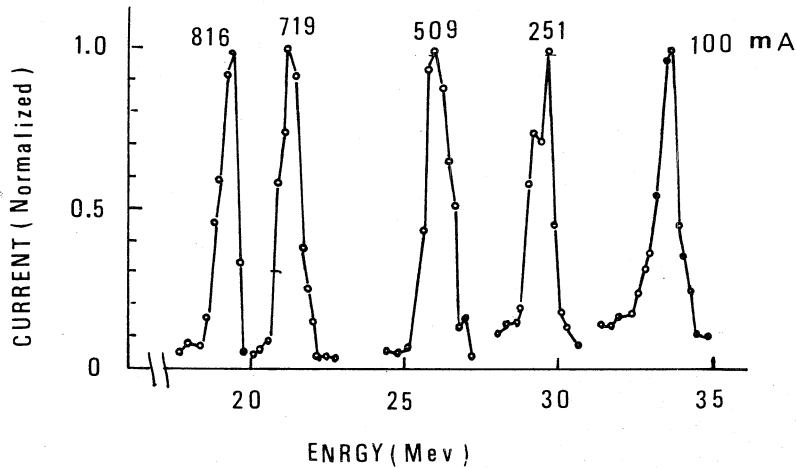


Fig. 8 Energy spectra measured at the end of injection system. Parameters indicated are injection current from the gun.

The ratio of the accelerated current measured at the end of the first accelerator guide to the injection current from the gun, as a capture efficiency, is plotted against the injection current in Fig. 9. At low currents the ratio is around 70%, and shows a tendency to decrease with the increase of the injection

current, but still remains around 60% at 800 mA injection current. In the figure the energy spread (FWHM/peak energy) is also plotted, and shows a slow increase with the increase of injection current. A question naturally arises if this is due to space charge effect. The measurements of the bunch width, therefore, were made, the results are shown in Fig. 10. There appears a tendency that the bunch width increases with the increase of the current showing that the longitudinal motion is affected with the injection current at these high currents.

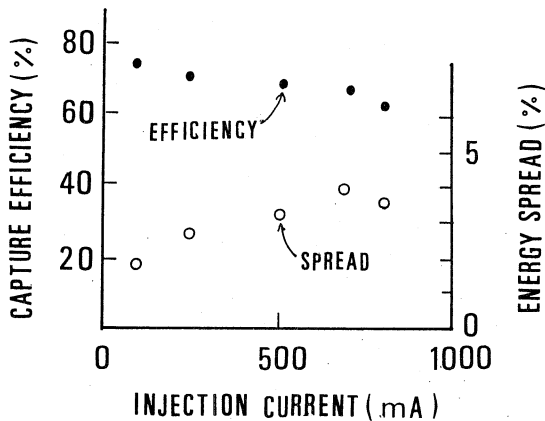


Fig. 9 Capture efficiency and energy spread for various injection currents.

REFERENCES

1. S. Ohsawa et al., Proc. 9th linac Meeting, Kyoto Univ., 1984, p.27 (in Japanese).
2. N. Kurosawa and Y. Hosono, *ibid*, p.33.
3. T. Ozaki et al., *ibid*, p.57.
4. S. Ohsawa et al., Proc. 8th Linac Meeting, INS Tokyo Univ., 1983, p.95 (in Japanese).
A. Asami et al., Proc. 9th Linac Meeting, Kyoto Univ., 1984, p.106 (in Japanese).
5. A. Asami et al., Proc. 4th Symp. Acc. Sci. and Tech. RIKEN, 1982, p.125.

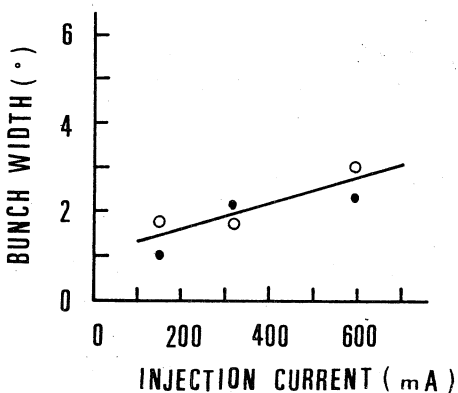


Fig. 10 Bunch width measured at various injection currents.